Non-linear higher order spectral solution of a moving load on a floating ice sheet

F. Bonnefoy [a] , M. Meylan [b] , P. Ferrant [a]

[a]Laboratoire de Mécanique des Fluides, CNRS UMR6598, Centrale Nantes, France

[b]Department of Mathematics, University of Auckland, New Zealand

1 Introduction

This paper is devoted to the non-linear response of an infinite ice sheet to a steady moving load in the time-domain using the higher order spectral method.

The linear problem has been well addressed (see *e.g.* Schulkes and Sneyd [7] in two dimensions) and predicts an infinite deflection at the critical speed. Experimental measurements of loads moving on ice *e.g.* [4] and [5] showed that there was good agreement between the linear theory and measurements except at the critical speed. While the experimental solutions presented a sharp peak close to the critical speed the solution remain finite.

Various theories have been proposed to better understand the solution close to the critical speed. Wang *et al.* [8] considered a visco-elastic model for the ice and showed that under these assumptions the response is finite for all speeds. Miles and Sneyd [9] considered the motion of an accelerating pressure (as opposed to one moving with constant velocity) and solved using a Fourier transform in space and a Laplace transform in time. They showed that the solution remains bounded if accelerated through the critical speed. Recently Parau and Dias [3] considered the two dimensional non-linear problem of a steadily moving load on ice at a subcritical speed. They transformed the problem into a dynamical system formulation and solved the obtained non-linear Schrödinger equation to find solitary wave solutions provided the speed was close to but smaller than the critical speed.

We consider the non-linear problem of the time-dependent motion of a moving load studied in more details in [1]. We show how the solution can be found using a modification of the higher order spectral method initially presented in [2] and [6]. This method uses a spectral expansion coupled with the fast Fourier transform to rapidly calculate the Dirichlet to Neuman map at the non-linear free-surface. The HOS method have proved useful for a variety of problems such as numerical wave tank modeling [11], freak wave formation [10] and incident wavefield estimations for seakeeping simulations [12]. The method is ideally suited to the problem of moving loads on ice by simply adding the non-linear flexural rigidity term in the dynamic free surface condition.

2 Modeling

An elastic plate floats on the surface of an inviscid and irrotational fluid which is infinite in the x-direction and has finite depth in the z direction. The ice sheet covers the entire water surface which is at $z = \xi$, where ξ is the displacement of the ice, and the bottom surface of

Email addresses: Felicien.Bonnefoy@ec-nantes.fr (F. Bonnefoy), meylan@math.auckland.ac.nz (, M. Meylan), Pierre.Ferrant@ec-nantes.fr (, P. Ferrant).

the fluid is at $z = -h$. The fluid is governed by Laplace's equation with a no flow condition at $z = -h$, and ϕ denotes the velocity potential in the fluid. At the ice-water interface we have a kinematic equation from the continuity of normal velocity and a dynamic equation from the pressure forces which are given by the non-linear Bernoulli equation and by the bending force of the plate and the pressure applied on the plate. The latter may be written as

$$\rho\phi_t + \frac{1}{2}\rho\left|\nabla\phi\right|^2 + \rho g\xi + D\Delta\frac{\Delta\xi}{\left(1+\left|\nabla\xi\right|^2\right)^{3/2}} = -p(x,t), \quad z = \xi \tag{1}$$

where ρ is the density of the plate, D is the bending rigidity of the plate and p is the applied external pressure. Note that we have set the inertia term to be zero.

We further scale the length by $L = (D/\rho g)^{1/4}$, time by $T = \sqrt{L/g}$ and the mass by $M = \rho L^3$. We also introduce the free surface potential $\phi_s(x,t) = \phi(x,\xi,t)$ and the vertical velocity $W(x,t) = \phi_z(x,\xi,t)$. We consider a line pressure travelling at speed U. This gives us $p\left(x,t\right) = \delta\left(x - Ut\right) f\left(t\right)$ where f is some arbitrary function. In a moving frame with velocity U the non-linear equations become

$$\partial_t\phi_s = U\partial_x\phi_s - \frac{1}{2}\left|\nabla\phi_s\right|^2 - \xi + \frac{1}{2}N\,W^2 - \Delta\left(\frac{\Delta\xi}{N^{3/2}}\right) - \delta\left(x\right)f\left(t\right), \quad z = \xi \tag{2}$$

$$\partial_t\xi = U\partial_x\xi + N\,W - \nabla\xi.\nabla\phi_s, \quad z = \xi \tag{3}$$

where $N = 1 + \left|\nabla\xi\right|^2$.

2.1 Higher order spectral method

The domain is supposed finite in the horizontal direction and a periodic condition is assumed at the horizontal boundaries. In such a case it is straightforward to express ξ and ϕ_s in a discrete Fourier domain. We solve these equations in time domain: assuming we know ϕ_s and ξ at time t, the free surface boundary conditions are used to evaluate the time derivatives of ξ and ϕ_s. In the latter conditions, the only remaining unknown is W, that is approximated by the high-order spectral (HOS) method. The latter was developed independently in [2] and [6] to simulate non-linear free-surface waves and uses a spectral expansion and the fast Fourier transform coupled with a modified Taylor series expansion to derive a very efficient way of computing the Dirichlet to Neumann map on the free surface (which is not assumed to lie on $z = 0$ as in the linear theory). The vertical velocity W is evaluated at order M in powers of ξ and related terms as NW and NW^2 are estimated consistently at order M as in [6].

2.1.1 Flexural rigidity

The non-linear flexural rigidity of the ice sheet is taken into account in the free surface equation for ϕ_{st} by the term $\Delta\left(N^{-3/2}\,\Delta\xi\right) = A\Delta^2\xi + 2\nabla A.\nabla\Delta\xi + \Delta A\,\Delta\xi$ where $A = N^{-3/2}$. For consistency with the HOS method, the three curvature related terms A, ∇A and ΔA are further expressed as Taylor expansions in ξ as follows

$$\begin{aligned} A &= 1 - \frac{3}{2}\left|\nabla\xi\right|^2 + \frac{15}{8}\left|\nabla\xi\right|^4 - \frac{35}{16}\left|\nabla\xi\right|^6\ldots & \mathbf{C} &= (\nabla\xi\,.\nabla)\nabla\xi \\ \nabla A &= B\,\mathbf{C} & B &= -3\left(1 - \frac{5}{2}\left|\nabla\xi\right|^2 + \frac{35}{8}\left|\nabla\xi\right|^4\ldots\right) \\ \Delta A &= \nabla B\,.\mathbf{C} + B\,\nabla\,.\mathbf{C} & \nabla B &= 15\left(1 - \frac{7}{2}\left|\nabla\xi\right|^2\ldots\right)\mathbf{C} \end{aligned}$$

The order of the three expansions is chosen adequately so that the flexural term is of order M in the dynamic boundary condition. For instance, the expansions presented above are valid for $M = 7$. Operators ∇ and Δ are evaluated in the Fourier space.

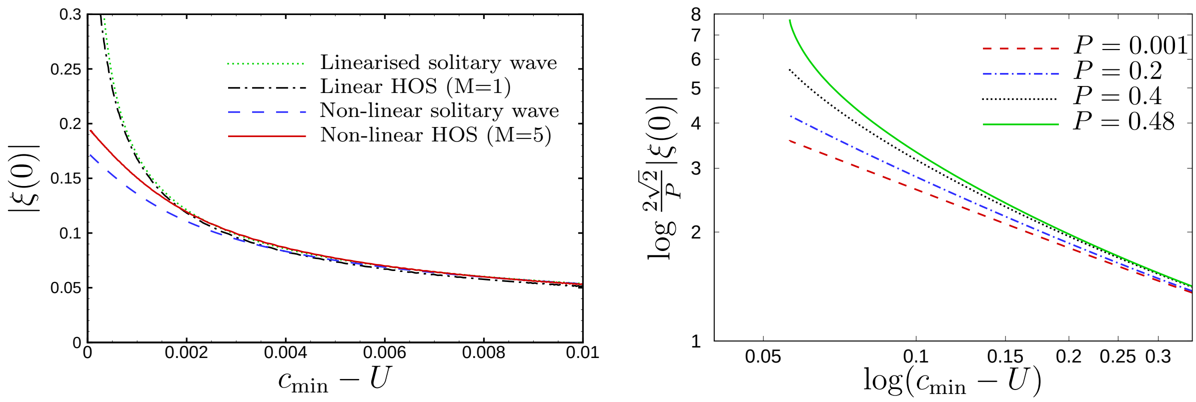

(a) Comparison with Parau and Dias results.

(b) Influence of the pressure forcing.

Figure 1: Maximum deflection at subcritical speeds.

2.1.2 Numerical model

The linear part of the equations 2 and 3 is analytically integrated in the moving frame except for the pressure term. The latter may be chosen with any given time evolution and we prefer to integrate its contribution numerically. Hence the pressure and non-linear evolution of the system are integrated numerically using a fourth-order Runge-Kutta Cash-Karp scheme with adaptive time step size.

The non-linear products involved in the free surface boundary conditions 2 and 3 are computed in the physical space. This leads to the well-known aliasing phenomenon which has to be addressed to preserve accuracy. In general, dealiased computations can be obtained by using spectra extended with zero padding. The number of collocation points in the physical space is then to be adequately determined for removing aliasing errors made on multiple products. The latter products are found in the free surface boundary conditions on the one hand, and within the iterative HOS obtention of W on the other hand. They are M-products at most (products involving M terms). Applying the half rule, the number of points to use in the physical space (N_x^d) to get a full dealiasing is $N_x^d = N_x(M+1)/2$.

3 Results

We begin here to compare our model to the solitary wave solution of Parau and Dias [3] when the velocity approaches the critical speed. Figure 1(a) shows the deflection measured at $x = 0$ against $c_{\min} - U$. In the first place we linearised their solitary wave solution for small pressure forcing and found a correct agreement with $M = 1$ in our model. Both solutions predict the linear blow up at $U = c_{\min}$. Secondly, the non-linear simulation with $M = 5$ and the solitary solution found a finite non-linear deflection for a pressure $P = 0.017$ at critical speed. Figure 1(b) shows the normalised deflection at $x = 0$ when the velocity is slowly increased from 0.8 to 1.25 ($c_{\min} = 1.32$) for higher pressures. The lowest pressure case (linear) clearly shows the one half inverse power law $(c_{\min} - U)^{-1/2}$ predicted by linear theory. When the pressure increases however, the maximum deflection departs from this kind of law. The closer the velocity to the critical speed the more pronounced the departure. With non-linear effects taken into account one may observe normalised deflections more than twice as high as the linear prediction.

Finally the model is used to predict the evolution of the deflection at critical speed with a pressure $P = 0.025$. Figure 2(a) shows the deflection at $x = 0$ against time. The linear $t^{1/2}$ increase is correctly reproduced until $t = 500$ when the non-linear effects kick in. The

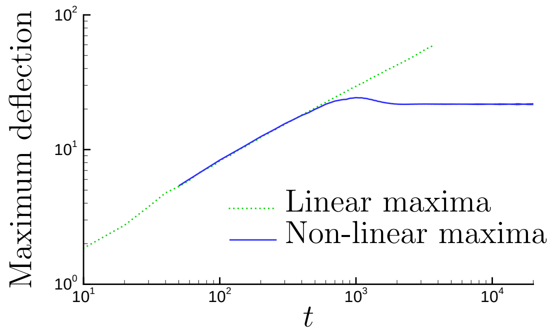

(a) Deflection at $x = 0$.

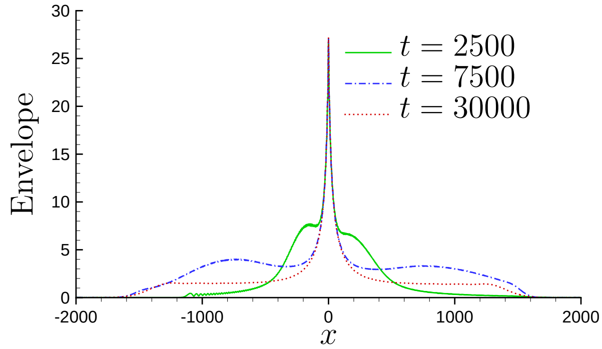

(b) Spatial envelope of the deflection.

Figure 2: Evolution of the deflection at critical speed $U = c_{\min}$.

deflection then reaches a non-linear stationary value at $t = 2000$. Figure 2(b) shows the steady state reached on each side of the line load.

The model developed here in two dimensions may be extended to three dimensions for comparisons with experiments.

References

[1] Bonnefoy, F., Meylan, M. H. & Ferrant P. 2008 Nonlinear higher-order spectral solution for a two-dimensional moving load on ice. *J. Fluid Mech.* In Press.

[2] Dommermuth, D. G. & Yue, D. K. 1987 A high-order spectral method for the study of non-linear gravity waves. *J. Fluid Mech.* **184**, 267–288.

[3] Parau, E. & Dias, F. 2002 Non-linear effects in the response of a floating ice plate to a moving load. *J. Fluid Mech.* **460**, 281–305.

[4] Takizawa, T. 1988 Response of a floating ice sheet to a steadily moving load. *J. Geophys. Res.*, **93**, 5100–5112.

[5] Squire, V. A., Robinson, W. H., Haskell, T. G. & Langhorne, P. J. 1985 Dynamic strain response of lake and sea ice to moving loads. *Cold Regions Sci. Technol.*, **11**, 123–129.

[6] West, B. J., Brueckner, K. A., Janda, R. S., Milder, D. M. & Milton, R. L. 1987 A new numerical method for surface hydrodynamics. *J. Geophys. Res.* **92** (C11), 11,803–11,824.

[7] Schulkes, R. M. and Sneyd, A. D. 1988 Time-dependent response of floating ice to a steadily moving load. *J. Fluid Mech.*, **186**, 25–46.

[8] Wang, K., Hosking, R. J. and Milinazzo, F. 2004 Time-dependent response of a floating viscoelastic plate to an impulsively started moving load. *J. Fluid Mech.*, **521**, 295–317.

[9] Miles, J. and Sneyd, A. D. 2003 The response of a floating ice sheet to an accelerating line load. *J. Fluid Mech.*, **497**, 435–439.

[10] Ducrozet, G., Bonnefoy, F., Le Touzé, D. & Ferrant P. 2007 3-D HOS simulations of extreme waves in open seas. *Nat. Hazards Earth System Sci.*, **7**, 109–122.

[11] Ducrozet, G., Bonnefoy, F., Le Touzé, D. & Ferrant P. 2006 Implementation and validation of nonlinear wave maker models in a HOS Numerical Wave Tank. *Int. J. Offshore Polar Eng.*, **16**(3), 161–167.

[12] Luquet, R., Ducrozet, G., Gentaz, L., Ferrant P., Alessandrini, B. 2007 Application of the SWENSE method to seakeeping simulations in irregular waves in *Proc.* 9^{th} *Num. Ship Hydro. Conf.*.